Macrocycles

DOI: 10.1002/anie.201410316

# Zethrene and Dibenzozethrene: Masked Biradical Molecules?**

*Ya-Chu Hsieh, Hau-Yu Fang, Yi-Ting Chen, Rong Yang, Chen-I Yang, Pi-Tai Chou,* Ming-Yu Kuo,* and Yao-Ting Wu**

*Dedicated to Lawrence T. Scott on the occasion of his 70th birthday*

***Abstract:*** *The syntheses, structures, and physical properties of dibenzozethrenes were explored. The results thus obtained were compared with those for zethrenes. Dibenzozethrenes were synthesized by the nickel-catalyzed cyclodimerization of 9-ethynyl-1-iodoanthracenes. The substituents in zethrene and dibenzozethrene twisted their backbones, and remarkably influenced their properties. Unlike closed-shell disubstituted derivatives, the parent zethrene and dibenzozethrene are singlet open-shell biradicals, which were studied by variable-temperature $^1$H NMR, ESR, SQUID and computational methods. Since substituents were observed to affect significantly the biradical properties, the relevant mechanisms were analyzed. The nonlinear optical performance of each of these compounds depends on its π-conjugation and biradical properties. Dibenzozethrenes have larger two-photon absorption cross-sections than zethrenes, as most strongly evidenced by the parent dibenzothrene [$\sigma_{max}$ = 4323 GM at 530 nm].*

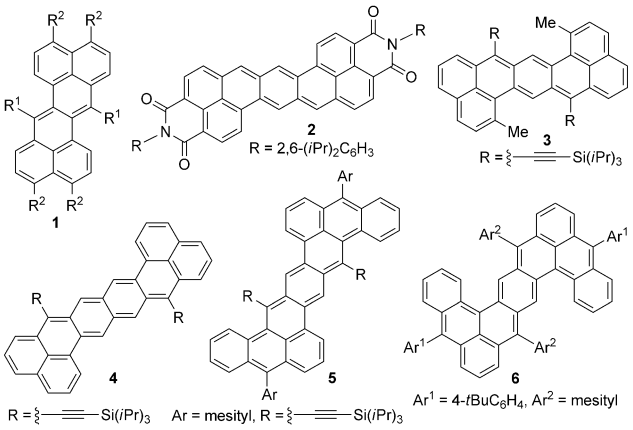


**D**ibenzo[*de*,*mn*]naphthacenes (zethrenes) **1**[1] and their π-extended derivatives, including the substituted heptazethrenes **2**[2]/**3**,[3] octazethrenes **4**,[3] and dibenzoheptazethrenes **5** and **6**,[4] which have remarkable chemical stability to contribute a non-Kekulé structure, bear two formal radical centers, and hence are well-suited to investigations of their biradical properties.[5] The compounds **2**, **4**, and **5** have been experimentally determined to have a significant open-shell biradical character, and exhibit unique optical and magnetic properties. The crossover from the Kekulé structure to the biradical structure is generally explained by the stabilization of the formation of Clar sextets,[6] which is a classic metric of the stability of closed-shell polycyclic aromatic hydrocarbons (PAHs).[7] This conclusion may be supported by a recent theoretical study of an unsubstituted zethrene series. Unlike heptazethrene, which has more sextets and, therefore, a strong singlet biradical character, zethrene can be practically treated as a closed-shell compound with a very tiny singlet biradical stabilization energy ($\Delta E_{br}$).[8] However, zethrene and its simple derivatives reportedly have a biradical character index ($y_0$) of approximately 40%.[1b,8b] An experimental investigation, which has not yet been conducted, could clarify these claims. In addition to stabilization by Clar sextets, substituents on the studied zethrene series **2**–**6** may strongly influence their biradical properties, although their parent compounds have not yet been synthesized. The effects of substituents in the heptazethrenes **2** and **3** are revealed by their properties: the former is open-shell, whereas the latter is closed-shell. Accordingly, this investigation explores the effects of substituents on the syntheses, structures, and physical properties of zethrenes and dibenzozethrenes. Substituents are connected to the positions, which bear the highest spin density in the parent compound.

An initial attempt to prepare the dibenzozethrene **8c** by the palladium-catalyzed cyclodimerization of 9-ethynyl-1-iodoanthracene (**7b**), in a manner similar to a protocol developed previously,[1e] failed, because a complex mixture was obtained and neither of the desired products (**8b** and **8c**; Scheme 1) was observed. Following systematic study of the

[*] Y.-C. Hsieh, H.-Y. Fang, Prof. Y.-T. Wu
Department of Chemistry, National Cheng Kung University
No. 1 Ta-Hsueh Rd., 70101 Tainan (Taiwan)
E-mail: ytwuchem@mail.ncku.edu.tw
Y.-T. Chen, Prof. P.-T. Chou
Department of Chemistry, National Taiwan University
No. 1, Sec. 4, Roosevelt Road, 10617 Taipei (Taiwan)
E-mail: chop@ntu.edu.tw
R. Yang, Prof. M.-Y. Kuo
Department of Applied Chemistry, National Chi Nan University
No. 1 University Rd., 54561 Puli, Nantou (Taiwan)
E-mail: mykuo@ncnu.edu.tw
Prof. C.-I. Yang
Department of Chemistry, Tunghai University
No. 181 Taichung-Kang Rd., Sec. 3, 40704 Taichung (Taiwan)

[**] Metal-Catalyzed Reactions of Alkynes. Part XVI. This work was supported by the Ministry of Science and Technology of Taiwan. We thank Prof. Sue-Lein Wang and Ms. Pei-Lin Chen (National Tsing Hua University, Taiwan) for the X-ray structure analyses. Prof. Hui-Lien Tsai (National Cheng Kung University) is acknowledged for a helpful discussion.

Supporting information for this article is available on the WWW under http://dx.doi.org/10.1002/anie.201410316.

  

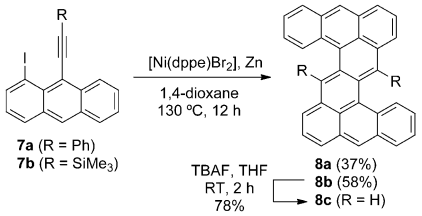


***Scheme 1.*** Synthesis of the dibenzozethrene **8c** and its derivatives. dppe = 1,2-bis(diphenylphosphanyl)ethane, TBAF = tetra-*n*-butylammonium fluoride, THF = tetrahydrofuran.

***Table 1:*** Selected bond lengths [Å] and twisted angles [°] of **1** and **8**.[a]

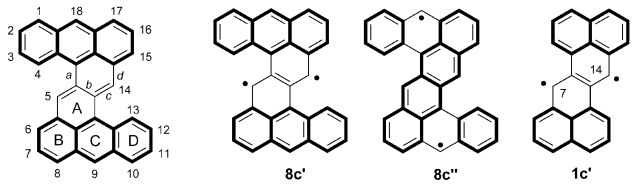


| Compound | | 8a | 8b | 8c | 1a | 1c |
|---|---|---|---|---|---|---|
| End-to-end Twist | | 45.4 | 59.9 | 18.3 | 42.4 | 0 |
| Degree of twisting | | 64.0 | 67.7 | 42.0 | 43.2 | 0 |
| Bond length | *a* | 1.474(1) | 1.458(2) | 1.480(4) | 1.469(4) | 1.480(1) |
| | *b* | 1.470(2) | 1.477(2) | 1.450(5) | 1.467(4) | 1.462(2) |
| | *c* | 1.373(1) | 1.378(2) | 1.367(4) | 1.378(4) | 1.364(1) |
| | *d* | 1.462(1) | 1.474(2) | 1.434(4) | 1.459(4) | 1.437(1) |
| HOMA | A | 0.02 | −0.04 | 0.28 | 0.09 | 0.16 |
| | B | 0.68 | 0.64 | 0.73 | 0.75 | 0.79 |
| | C | 0.74 | 0.74 | 0.74 | 0.80 | 0.85 |
| | D | 0.67 | 0.58 | 0.67 | – | – |

[a] The end-to-end twist is determined from the torsion angle of C17-C16-C8-C7 in the naphthacene moiety. The degree of twisting of **8** or **1** is analyzed by the dihedral angle between two periphery anthryl or naphthyl planes, respectively. The structure of **1a** and **1c** were obtained from Ref. [1e]. HOMA values 1 and 0 indicate aromaticity and no-aromaticity, respectively.

reaction conditions, **8a** and **8b** were easily synthesized from **7a** and **7b**, respectively, with catalysis by [Ni(dppe)$Br_2$]. The structure of **8b** is more twisted than that of **8a** (Table 1), but the former was obtained more efficiently than the latter. The low solubility of **8a** in common organic solvents was probably responsible for the low yield, since some of the material was irreversibly lost during chromatography. Treatment of **8b** with tetra-*n*-butylammonium fluoride gave **8c** in 78% yield. Although the stabilities of **8** were not closely examined, substituted products were more stable than the parent compound. An aerobic solution of **8c** placed in the dark at room temperature was stable for over two weeks, after which some new signals appeared in its $^1$H NMR spectrum.

The molecular structures of **8a**, **8b**, and **8c** were analyzed by X-ray crystallography, and their structural data are summarized in Table 1 and Table S2 (see the Supporting Information).[9] All of the structures deviate substantially from planarity, and their degrees of twisting ($\theta$), measured as the dihedral angle between two periphery anthracenes, were determined to be 64.0°, 67.7°, and 42.0° for **8a**, **8b**, and **8c**, respectively. A PAH very rarely has a highly twisted backbone like that of **8b**. The parent **8c** has around 2–3 pm shorter *b* and *d* bonds than **8a** and **8b**. The HOMA (harmonic oscillator model of aromaticity)[10] analysis reveals that the central naphthyl bridges (rings A) in **8c** and **8a**/**8b** are weak and non-aromactic, respectively. Similar features were also observed in **1a** ($R^1$ = Ph, $R^2$ = H) and **1c** ($R^1 = R^2$ = H). The latter has a shorter *d* bond and slightly stronger aromaticity of the central naphthyl bridge than the former, but the shortening of the *b* bond is less significant. These geometric findings and results concerning aromacticity suggest the existence of biradical resonance forms, which are denoted as **1c′** and **8c′**. These results are also consistent with their biradical character indices ($y_0$) which are estimated using the spin-projected unrestricted Hartree–Fock (PUHF) method: **1c** and **8c** are singlet biradical molecules with index values of 0.36 and 0.48, respectively, whereas **1a**, **8a**, and **8b** have a closed-shell ground state. Through-bond interactions between the substituent and the backbone in **1a**, **8a**, and **8b** seem to be unimportant because the lengths of the σ bond are not atypical.

Unlike the heptazethrene **3**, octazethrene **4**,[3] and bisphenalenyl derivatives,[11] which form one-dimensional infinite chains by tail-to-head interactions, molecules of **8c** stack in columns along the *c* axis, as presented in Figure 1. Within a columnar stack, any two adjacent molecules, arbitrarily

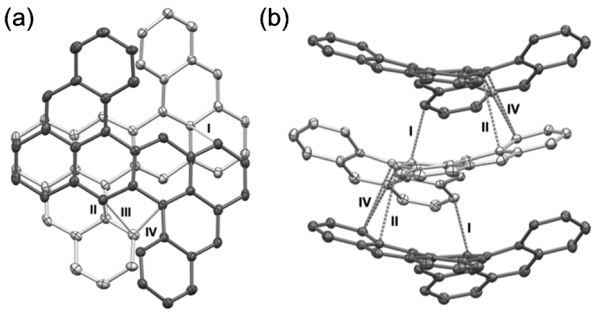


***Figure 1.*** Crystal packing in **8c**. a) Along the *b* axis. b) Along the *c* axis. Only carbon atoms are shown for clarity. Non-conducted C–C distances in [Å]: **I**: 3.277; **II**: 3.305; **III**: 3.328 and **IV**: 3.302.

denoted as A and B (not shown), with opposite molecular orientations form a π-dimer with effective π/π surface overlap mainly between their naphthacene moieties. Owing to the nonplanar conformation of the naphthacene cores and the nonperfect overlap between them, the shortest distance between A and B is difficult to quantify accurately. However, the separation between the two closest A molecules is 7.644 Å, and the shortest carbon–carbon contact distance within a π-dimer was determined to be 3.277 Å, which is smaller than the sum of the van der Waals radii of two carbon atoms (3.40 Å).[12] Although a naphthacene moiety contains a significant SOMO distribution, the surface overlap within

  

a π-dimer should not be treated as intermolecular covalent π-bonding, which is often observed in bisphenalenyls (see below).[11] Notably, the π/π stacking in zethrene **1c** is inefficient, and that in the substituted compounds **1a**, **8a** and **8b**, is insignificant.

$^1$H NMR spectra of **1a**, **1c**, **8a**, **8b**, and **8c** in $CDCl_3$, obtained at room temperature, exhibit well-resolved resonance signals. Broadening of the **8c** signal was not observed when the measurement was conducted in $CD_2Cl_2$, [$D_8$]THF, and [$D_8$]toluene at room temperature or in [$D_8$]toluene at 373 K. The absence of the expected line broadening of **1c** and **8c** should be caused by conformational motions, which are significant for molecules in solutions, and decrease the biradical character index (see below).

Electron spin resonance (ESR) measurements were made using powder samples. All substituted compounds, **1a**, **8a**, and **8b**, are ESR inert, even at 300 K, thus manifesting their closed-shell properties. Similar to **4**,[3] **5**,[4] and quarteranthene,[14] both **1c** and **8c** exhibited featureless broad signals centered at $g = 2.0026$ and 2.0005, respectively (Figure 2 and the Supporting Information), and $\Delta M_s = \pm 2$ transitions were not observed. These spectral features were caused by the weak spin–spin dipole interaction within the molecules, the long-distance separation between two radicals, and the extended spin-delocalization. Unlike many biradicals, such as **4**,[3] quarteranthene,[13] and others,[14] according to the VT ESR measurements at 150–300 K, **1c** and **8c** exhibited decreasing ESR intensity as the temperature increased. Conformational motions presumably govern this phenomenon (see below).

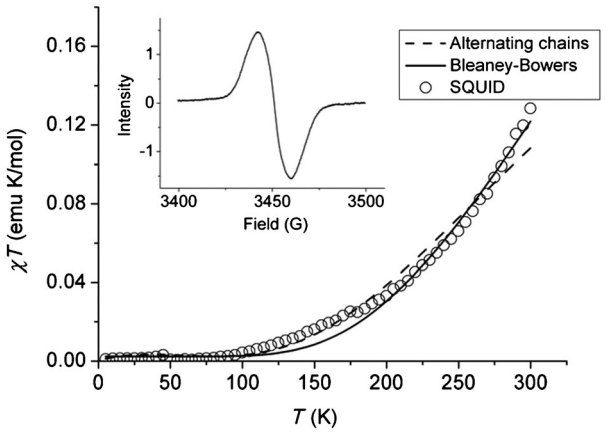


***Figure 2.*** $\chi T$–$T$ plot of powdered **8c**. The theoretical curves are fitted according to the Bleaney–Bowers equation (parameters: $g = 2.0036$, $J = -372.5$ cm$^{-1}$ and paramagnetic impurity = 0.315 %) and the alternating Heisenberg chain model (parameters: $g = 2.0036$, $J_{intra} = -248.3$ cm$^{-1}$, $J_{inter} = -3.25$ cm$^{-1}$, and impurity spin contamination = 0.043 %). Inset: A ESR spectrum of powdered **8c** measured at room temperature.

The temperature-dependent magnetic susceptibility data on powdered **8c** at 5–300 K were collected using a superconducting quantum interference device (SQUID) magnetometer. Figure 2 plots $\chi T$ as a function of $T$. As the temperature is decreased, $\chi T$ approaches a minimum of close to zero at around 50 K and then increases slightly. At room temperature, **8c** has a $\chi T$ value (0.12 emu K mol$^{-1}$) which is smaller than that of two uncorrelated spins, but larger than those of **4** and **5**.[3,4] Careful fitting of the observed data using the Bleaney–Bowers equation yielded the singlet–triplet energy gap $\Delta E_{S\text{-}T}$ ($2J$) as $-2.13$ kcal mol$^{-1}$.[15] This result demonstrates that **8c** has a singlet biradical ground state with the two weakly coupled unpaired electrons. Analyses based on the alternating Heisenberg chain model[16] yielded a similar result—a very small value of $\Delta E_{S\text{-}T}$ ($-1.42$ kcal mol$^{-1}$) and a negligible intermolecular interaction to biradical properties, presumably owing to the long intermolecular distance (around 3.8 Å) between two closest naphthacene moieties within a column stack, as revealed by the X-ray crystallographic analysis described above. Although **1c** is ESR-active, its values of $\chi T$ are extremely tiny and the plot of $\chi T$ against $T$ is not reproducible, even by making measurements in different types of sample holders. This result arises from the very small values of the magnetic susceptibility, and are comparable to experimental errors.

Electrochemical properties of **1** and **8** were studied using cyclic voltammetry. The cyclic voltammograms of **8** included four redox waves with two oxidation and two reduction potentials (Table 2; see Table S3 in the Supporting Information). The second oxidation and reduction signals are irreversible. The irreversibility of the redox waves reveals low thermodynamic stabilities of the divalent ionic species. The less π-conjugated **1a** and **1c** present three redox waves with one oxidation and two reduction potentials in their cyclic voltammograms, and the first oxidation and reduction potentials are reversible. As expected, the compounds **8** have lower oxidation and reduction potentials than **1**. Within compound classes, the electrochemistry of the **1a**/**1c** couple, as well as that of **8a**/**8c** are similar, with the exception of the first reduction potential. The first reduction potential for unsubstituted **1c** and **8c** is significantly lower than that of **1a** and **8a**, respectively. The electrochemical HOMO–LUMO gaps ($E_g^E$) of the compounds in Table 2 follow the order **1a** > **1c** > **8a** ≈ **8b** > **8c**. Importantly, the $E_g^E$ value for the open-shell **8c** (1.81 eV) greatly exceeds that for the closed-shell **3** (1.46 eV).

***Table 2:*** Selected physical properties of the zethrenes **1** and dibenzozethrenes **8**.[a]

| | $\lambda_{abs}$ [nm] | $\lambda_{em}$ [nm] | $E_{1/2}^{ox}$ [V] | $E_{1/2}^{red}$ [V] | $E_g^E$ [eV] | $\sigma_{max}$ [GM][b] |
|---|---|---|---|---|---|---|
| **1a** | 523 | 571 | 0.30 | −1.93, −2.06[c] | 2.22 | 265 |
| **1c** | 543 | 574 | 0.30 | −1.69, −2.06[c] | 2.00 | 373 |
| **8a** | 582 | 662 | 0.19, 0.52[c] | −1.79, −1.84[c] | 1.97 | 3438 |
| **8b** | 586 | 672 | 0.25, 0.61[c] | −1.70, −1.92[c] | 1.96 | 2885 |
| **8c** | 592 | 683 | 0.22, 0.55[c] | −1.58, −1.83[c] | 1.81 | 4323 |

[a] The electrochemical and photophysical properties of **1** and **8** were measured in $CH_2Cl_2$. $E_{1/2}^{ox}$ and $E_{1/2}^{red}$ are half-wave potentials of the oxidative and reductive waves measured in $CH_2Cl_2$, respectively, with potentials vs $Fc/Fc^+$ couple. $Eg^E$: The electrochemical HOMO–LUMO gap. [b] $\sigma_{max}$ is the maximum TPA cross section at the wavelength of 530 nm. [c] For an irreversible wave, the potential was determined by its onset value.

  

These results are not consistent with a suggestion that a small $E_g^E$ value is critical to the formation of a singlet open-shell biradical.[6,17]

The photophysical properties of zethrene and dibenzozethrene are influenced by substituents/conformation and π-conjugation of their backbones, but the π-conjugation is critical (Table 2; see Table S4 in the Supporting Information). In contrast to **1**, the compound class **8** with a more extended π-system exhibited significantly red-shifted absorption and emission bands by approximately 50 and 110 nm, respectively. Within a compound class, twisting the backbone causes the absorption and/or emission bands to shift hypsochromically. Phenyl or trimethylsilyl substituents are not significantly involved in the π-system of a backbone. Notably, the compounds in Table 2 do not have absorption bands above $\lambda = 800$ nm.

The nonlinear optical properties of **1** and **8** were measured using a method based on two-photon-induced fluorescence with excitation wavelengths of $\lambda = 940$–$1420$ nm, and measurements were not perturbed by one-photon absorption. This investigation provides information that elucidates the correlations between the two-photon absorption (TPA) properties and structure (Tables 2; see Table S5 in the Supporting Information). The TPA cross-sections of these compounds depend on their π-conjugation, conformation, and biradical properties, but the first is more important than the latter two. TPA cross-sections ($\sigma_{max}$) of **8** are around one order of magnitude larger than those of **1**. Within each compound class, the parent compound, which is a singlet biradical with a less twisted conformation, has the largest $\sigma_{max}$ value. As a result, **8c** has a highest value ($\sigma_{max} = 4323$ GM at 530 nm).

Presumably, the biradical properties of **1** and **8** are affected by their structures and $\Delta E_{br}$. The main structural differences between the closed-shell **1a**/**8a** and open-shell **1c**/**8c** are their degrees of twisting ($\theta$) and the intermolecular interaction in crystals. These factors can be analyzed theoretically and the results thus obtained compared with experimental results. The optimized structures of **8a–c** were obtained using density-functional theory at the CAM-B3LYP/6-31G** level, and the results agree closely with crystallographic analysis (Table S2). The $\Delta E_{br}$ value for the optimized **8c** was theoretically determined to be around $-0.4$ kcal mol$^{-1}$, thus indicating that the singlet open-shell biradical form is more stable than the closed-shell structure. Theoretical studies of the dynamic behaviors of **8c** are performed to elucidate relationships among the conformation, relative potential energy ($\Delta E_p$) and $y_0$ value (see Figure S3 in the Supporting Information). The nonplanar conformation is characterized by the degree of twisting ($\theta = 23$–$75°$), and $\Delta E_p$ of the optimized structure ($\theta = 42°$) is used as a reference. Deformation of the structure does affect the biradical character index ($0.54 \geq y_0 \geq 0.42$). For example, a small change of the optimized conformation ($\Delta\theta = +5°$) decreases the value of $y_0$ from 0.48 to 0.43, and this deformation requires only around 0.7 kcal mol$^{-1}$. This effect may explain the absence of the expected line broadening in $^1$H NMR spectrum and decreasing ESR intensity as the temperature increases. When **8c** is highly twisted ($75° \geq \theta \geq 42°$), $y_0$ is almost constant, with a value of about 0.43, and the intramolecular interaction between two radicals is negligible. The degree of twisting of both the closed-shell **8a** ($\theta = 64°$) and **8b** ($\theta = 68°$) falls in this range, thus suggesting that the twisted conformation does not critically affecting the biradical properties. Notably, the inversion between the two "enantiomers" of **8c** in the gas phase proceeds via a nonplanar transition structure, and the barrier to this energetically favorable route is approximately 10.8 kcal mol$^{-1}$ (see Figure S2 in the Supporting Information). Although the mechanism by which the substituents affect the biradical properties of **8** is still unknown, the present studies exclude the following three possibilities: 1) twisting of backbone, 2) intermolecular interactions in crystals, and 3) through-bond interactions between the substituent and the backbone.

The optimized structure of **1c** is consistent with the experimentally determined bond lengths and bond angles, but it has a twisted conformation in the gas phase, rather than the planar structure of the crystal. The dihedral angle between two periphery naphthyl planes was determined to be 13.2°. The intrinsic reaction coordinate (IRC) confirmed that the planar structure is a transition state in the inversion process between the two "enantiomers" of the optimized structure, and the barrier is only around 0.1 kcal mol$^{-1}$. If the theoretically determined structure of **1c** is real, then its planar conformation in the solid state should be caused by the crystal packing. The calculated $y_0$ values for the optimized and planar structures are determined to be 0 and 0.36, respectively. The biradical properties of **1c** depend strongly on the conformation: **1c** becomes a closed-shell compound when $\theta$ exceeds 9° (see Figure S4 in the Supporting Information). Accordingly, the closed-shell character of **1a** is caused by structural deformation. As in previous investigations,[8] **1c** has a tiny $\Delta E_{br}$ (approximately $-10^{-4}$ kcal mol$^{-1}$) with a barely significant biradical character.

The theoretical investigations of the spin density distributions of **1c** and **8c** herein indicate that the spin density in the former is much smaller than that in the latter (see Figure S1 in the Supporting Information). The studies herein also leave open the question of whether Clar's aromatic sextet rule can be used to predict the dominant resonance form of biradical molecules. For example, **1c′** with two sextets is the most stable resonance form with the highest spin density at C7/14. However, **8c″** with three sextets should be more stable than **8c′** with two sextets, but the former molecule has the highest spin density at C5/14 (Figure S1).

In conclusion, substituents in zethrene and dibenzozethrene strongly influence their structures and physical properties. In contrast to closed-shell disubstituted derivatives **1a**, **8a**, and **8b**, the parent zethrene **1c** and dibenzozethrene **8c** are singlet open-shell biradicals, and the latter has a much stronger biradical character than the former. Consequently, the properties of the unsubstituted and π-extended zethrene series may differ remarkably from those of their substituted derivatives. Moreover, **8c** has some different physical properties, including a broader ESR signal, the declining ESR intensity with increasing temperature, a higher value of $\chi T$ at room temperature, and a larger electrochemical HOMO–LUMO gap ($E_g^E$) than the extensively studied zethrene-based biradicals **4** and **5**. The extension of this facile synthetic

  

approach to synthesize more extended derivatives, and investigations of their properties are in progress.

Received: October 21, 2014
Revised: November 24, 2014
Published online: January 29, 2015

**Keywords:** density functional calculations · dimerization · macrocycles · nickel · radicals

[1] For recent examples, see: a) Z. Sun, J. Wu, *J. Org. Chem.* **2013**, *78*, 9032; b) D. Hibi, K. Kitabayashi, A. Shimizu, R. Umeda, Y. Tobe, *Org. Biomol. Chem.* **2013**, *11*, 8256; c) L. Shan, Z. Liang, X. Xu, Q. Tang, Q. Miao, *Chem. Sci.* **2013**, *4*, 3294; d) Z. Sun, K.-W. Huang, J. Wu, *Org. Lett.* **2010**, *12*, 4690; e) T.-C. Wu, C.-H. Chen, D. Hibi, A. Shimizu, Y. Tobe, Y.-T. Wu, *Angew. Chem. Int. Ed.* **2010**, *49*, 7059; *Angew. Chem.* **2010**, *122*, 7213; f) R. Umeda, D. Hibi, K. Miki, Y. Tobe, *Org. Lett.* **2009**, *11*, 4104; For review, see: g) R. Umeda, D. Hibi, K. Miki, Y. Tobe, *Pure Appl. Chem.* **2010**, *82*, 871.

[2] Z. Sun, K.-W. Huang, J. Wu, *J. Am. Chem. Soc.* **2011**, *133*, 11896.

[3] Y. Li, W.-K. Heng, B. S. Lee, N. Aratani, J. L. Zafra, N. Bao, R. Lee, Y. M. Sung, Z. Sun, K.-W. Huang, R. D. Webster, J. T. L. Navarrete, D. Kim, A. Osuka, J. Casado, J. Ding, J. Wu, *J. Am. Chem. Soc.* **2012**, *134*, 14913.

[4] Z. Sun, S. Lee, K. H. Park, X. Zhu, W. Zhang, B. Zheng, P. Hu, Z. Zeng, S. Das, Y. Li, C. Chi, R.-W. Li, K.-W. Huang, J. Ding, D. Kim, J. Wu, *J. Am. Chem. Soc.* **2013**, *135*, 18229.

[5] Biradical is defined as the two electrons within a molecule act (nearly) independently. For details, see: a) IUPAC Compendium of Chemical Terminology, release 2.3.2; International Union of Pure and Applied Chemistry (IUPAC), Research Triangle Park, NC, **2012**, pp. 168. Recent reviews: b) M. Abe, *Chem. Rev.* **2013**, *113*, 7011; c) Y. Morita, S. Nishida in *Stable Radicals* (Ed.: R. G. Hicks), Wiley, Chichester, **2010**, pp. 81; d) Z. Sun, J, Wu, *J. Mater. Chem.* **2012**, *22*, 4151; e) Z. Sun, Z. Zeng, J. Wu, *Acc. Chem. Res.* **2014**, *47*, 2582.

[6] A. Konishi, Y. Hirao, M. Nakano, A. Shimizu, E. Botek, B. Champagne, D. Shiomi, K. Sato, T. Takui, K. Matsumoto, H. Kurata, T. Kubo, *J. Am. Chem. Soc.* **2010**, *132*, 11021.

[7] E. Clar, *The aromatic sextet*, Wiley, London, **1972**.

[8] The stabilization energy of the singlet biradical ($\Delta E_{br}$) is expressed as $\Delta E_{br} = E_{os} - E_{cs}$, where $E_{os}$ and $E_{cs}$ are the potential energies of the singlet open-shell and closed-shell states, respectively. A compound with $\Delta E_{br} \geq 0$ is closed-shell. For details, see: a) J. L. Zafra, R. C. G. Cano, M. C. R. Delgado, Z. Sun, Y. Li, J. T. L. Navarrete, J. Wu, J. Casado, *J. Chem. Phys.* **2014**, *140*, 054706; b) S. Marković, S. Radenković, Z. Marković, I. Gutman, *Russ. J. Phys. Chem. A* **2011**, *85*, 2368.

[9] CCDC 1029016 (**8a**), 1029017 (**8b**), and 1029018 (**8c**) contain the supplementary crystallographic data for this paper. These data can be obtained free of charge from The Cambridge Crystallographic Data Centre via www.ccdc.cam.ac.uk/data_request/cif.

[10] a) J. Kruszewski, T. M. Krygowski, *Tetrahedron Lett.* **1972**, *13*, 3839; For a review on HOMA, see: b) T. M. Krygowski, M. K. Cyrański, *Chem. Rev.* **2001**, *101*, 1385.

[11] a) A. Shimizu, M. Uruichi, K. Yakushi, H. Matsuzaki, H. Okamoto, M. Nakano, Y. Hirao, K. Matsumoto, H. Kurata, T. Kubo, *Angew. Chem. Int. Ed.* **2009**, *48*, 5482; *Angew. Chem.* **2009**, *121*, 5590; b) T. Kubo, A. Shimizu, M. Sakamoto, M. Uruichi, K. Yakushi, M. Nakano, D. Shiomi, K. Sato, T. Takui, Y. Morita, K. Nakasuji, *Angew. Chem. Int. Ed.* **2005**, *44*, 6564; *Angew. Chem.* **2005**, *117*, 6722; for a discussion on covalent bonding interactions in bisphenalenyls, see: c) L. Huang, M. Kertesz, *J. Am. Chem. Soc.* **2007**, *129*, 1634.

[12] a) L. Pauling, *The Nature of the Chemical Bond*, 3rd ed., Cornell University Press, Ithaca, **1960**. According to the Zefirov's definition, the sum of van der Waals radii of two carbon atoms is 3.42 Å, see: b) Y. V. Zefirov, *Crystallogr. Rep.* **1997**, *42*, 865.

[13] A. Konishi, Y. Hirao, K. Matsumoto, H. Kurata, R. Kishi, Y. Shigeta, M. Nakano, K. Tokunaga, K. Kamada, T. Kubo, *J. Am. Chem. Soc.* **2013**, *135*, 1430.

[14] a) D. Luo, S. Lee, B. Zheng, Z. Sun, W. Zeng, K.-W. Huang, K. Furukawa, D. Kim, R. D. Webster, J. Wu, *Chem. Sci.* **2014**, *5*, 4944; b) Z. Zeng, M. Ishida, J. L. Zafra, X. Zhu, Y. M. Sung, N. Bao, R. D. Webster, B. S. Lee, R.-W. Li, W. Zeng, Y. Li, C. Chi, J. T. L. Navarrete, J. Ding, J. Casado, D. Kim, J. Wu, *J. Am. Chem. Soc.* **2013**, *135*, 6363; c) S. Das, S. Lee, M. Son, X. Zhu, W. Zhang, B. Zheng, P. Hu, Z. Zeng, Z. Sun, W. Zeng, R.-W. Li, K.-W. Huang, J. Ding, D. Kim, J. Wu, *Chem. Eur. J.* **2014**, *20*, 11410.

[15] B. Bleaney, K. D. Bowers, *Proc. R. Soc. London Ser. A* **1952**, *214*, 451.

[16] D. C. Johnston, R. K. Kremer, M. Troyer, X. Wang, A. Klümper, S. L. Bud'ko, A. F. Panchula, P. C. Canfield, *Phys. Rev. B* **2000**, *61*, 9558.

[17] K. Ohashi, T. Kubo, T. Masui, K. Yamamoto, K. Nakasuji, T. Takui, Y. Kai, I. Murata, *J. Am. Chem. Soc.* **1998**, *120*, 2018.

  